Proceeding of the IEEE
International Conference on Robotics and Biomimetics
Dali, China, December 2019

Preliminary Study on Shape Sensing for Continuum Robot Affected by External Load Using Piecewise Fitting Curves

Hao Guo. Feng Ju, *Member, IEEE*. Bai Chen*.

***Abstract*— This paper proposes a new method of shape sensing for continuum robot affected by external load using piecewise fitting curves. This scheme will integrate posture sensors into continuum robot, and then the shape is reconstructed by piecewise fitting Bézier curves. The simulation analysis is used to analyze the curvature and radius change of each section of the continuum robot, when the end of the bending continuum robot with constant curvature is subjected to external load. The layout scheme of sensors is determined according to the curvature and radius of each section. The shape of image recognition is compared with the shape of piecewise fitting cubic Bézier curves in simulation. The maximum tracking error is 1.4 mm and the minimum tracking error is 0.006 mm. The simulation results verify the accuracy and feasibility of this method.**

Keywords—Continuum robot，shape sensing，external load，piecewise fitting curves

I. INTRODUCTION

Continuum robots can be better adapted to the narrow, unknown working environment by changing its shape, which have attracted more attention. However, compared with discrete robots, continuum robots do not have joints to install encoders, potentiometers or other traditional sensors to collect feedback information. At present, most continuum robots do not have their own shape perception ability and can not form closed-loop control. Therefore, it is very important to study a method that can quickly detect the shape of continuum robots.

In recent years, the shape sensing methods for continuum robots mainly focus on the following three categories: (1) Image recognition; (2) Intelligent materials; (3) Special sensors.

(1) Image recognition

The shape sensing method based on image recognition detection is the most mature method in existing applications. There are two main types of this method. One is to use high-speed camera to acquire the shape of continuum robot in open space. Hannan.M.W and Walker.I.D [1] use monocular camera to acquire the image of continuum robot, and then use the corresponding algorithm to get the shape of the robot. Binocular vision [2][3] and trinocular vision [4] are also applied in continuum robot shape sensing. The other is to use medical imaging technology to acquire the shape of continuum robot in closed space (mainly in the human body). The most commonly used medical imaging techniques are X-ray [5], CT, and MRI [6]. Both of the above methods have the disadvantage of long time consumed in image processing and can not meet the real-time The latter method has a high risk of using radiation.

(2)Intelligent materials

The shape sensing method based on intelligent materials mainly focus on polyvinylidene fluoride (PVDF) and ion exchange polymerized metal material (IPMC) [7].There are also some other materials used in this filed, such as conductive textile [8] and rubber diffraction grating sheet [9]. Yoel Shapiro [10] uses an embedded piezoelectric film made of PVDF to track the flexible software robot in real time and realize 2-D shape reconstruction. Bahramzadeh [11] integrates IPMC materials with cantilever beams and calculated the bending angle changes of the beams by the upper computer. This method will lead to complex configuration of robots and it also has not yet been focused on the shape sensing of continuum robots in the 3D space.

(3)Special sensors

The shape sensing method based on special sensors is popular research field. Special sensors are mainly focused on electromagnetic sensor and fiber prague grating (FBG) sensor. Zheng Li and Shuang Song[12] develop a shape sensing system using NDI electromagnetic tracker. The position and posture signals of the end of the continuum robot are detected by the electromagnetic sensors, and the shape will be reconstructed by fitting Bézier curve. NDI electromagnetic tracker is widely used in the field of medical robots, but it needs additional electromagnetic generator. Shuang Song [13] uses permanent magnet as the magnet source and the tracking target of the end of continuum robot. The position and posture of the end of the robot are obtained by measuring the magnetic flux density through the magnetic sensor array platform. and then the shape can be fitted according to Bézier curve. This method also requires adding additional detection equipment outside the robot. Davis.M.A detects the deformation of cantilever beam by wavelength division multiplexing of FBG sensor. In the way of [14], FBG sensors are embedded into the continuum robot itself. The strain of the continuum robot during bending can be calculated by measuring the change of bragg wavelength. And then the curvature of each grating node of continuum robot is deduced to reconstruct the 2D shape.

*Resrach supported by National Natural Science Foundation of China (No. 51575256) and (No. 61973335), Natural Science Foundation of Jiangsu Province under Grant BK20191272, and "the Fundamental Research Funds for the Central Universities. NO. NS2018033".

Hao Guo is currently a PhD degree candidate at the College of Mechanical and Electrical Engineering, Nanjing University of Aeronautics and Astronautics, Nanjing, Jiangsu Province, China. (e-mail: wulinguohao@163.com).

Feng Ju is currently an Associate Professor in the School of Mechanical and Electrical Engineering, Nanjing University of Aeronautics and Astronautics. Nanjing, Jiangsu Province, China. (e-mail: juf@nuaa.edu.cn).

Bai Chen* is currently a Professor and PhD candidate supervisor at the College of Mechanical and Electrical Engineering, Nanjing University of Aeronautics and Astronautics, Nanjing, Jiangsu Province, China. (phone: +86 13951726981; fax: 025-84892503; e-mail: chenbye@nuaa.edu.cn).

978-1-7281-6321-5/19//$31.00 ©2019 IEEE

Roesthuis [15][16] expands the shape sensing method baesd on FBG sensors in 3D space. But the measurement range of FBG sensor is limited, so it can only measure small deformation of continuum robot. Although [17] and [18] expand the application in large deformation by changing the layout of FBG sensors, the processing difficulty and the cost of using FBG sensors are greatly increased due to the fragility of grating nodes.

At present, continuum robot shape sensing is mostly focused on natural bending without the influence of external load. In this situation, the bending of continuum is constant curvature. When the end of the continuum robot is subjected to external load, it no longer meets the condition of constant curvature bending. [19] proposes a novel dual-layer control architecture to compensate for this deflection during trajectory tracking By considering the tip deflection resulting from the external load. However, only a few researchers are engaged in the research of shape sensing methods for continuum robot affected by external load.

In this paper, a shape sensing method for externally loaded continuum robot is proposed. this scheme will integrate posture sensors into continuum robot, and then the shape of continuum robot affected by external load is reconstructed by fitting Bézier curve several times. Because the bending curvature of different sections will change when the end of the continuum robot is subjected to external load. So what this paper focuses is how to arrange sensors according to the simulation analysis of continuum robot affected by external load to ensure the simplicity of configuration and the accuracy of shape sensing.

II. Structure and Shape Reconstruction Method

A. Structure

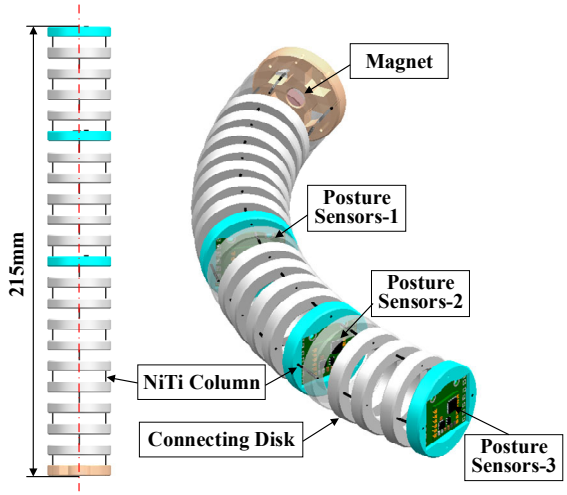

Figure 1. Overall sketch of the continuum robot (include three posture sensors and one permanent magnet). The continuum robot consists of 22 cylindrical connecting disks made of resin material and 21 pairs of 5-mm-long NiTi columns. Each connecting disk has a thickness of 5 mm and a diameter of 30 mm. The length of the single section is 215mm.

In order to solve the problem that traditional continuum robot have twisting problems in their central located flexible back-bone, [20] proposes a new structure. In this paper, the posture sensors and magnet are integrated into the continuum robot with this new structure to detect its shape affected by external load.

As shown in Figure 1, the continuum robot consists of 22 cylindrical connecting disks made of resin material and 21 pairs of 5-mm-long NiTi columns. Each connecting disk has a thickness of 5 mm and a diameter of 30 mm. The length of the single section is 215mm, which can realize flexible movement in 3D space. Posture sensors mainly include gyroscope sensor, three-axis acceleration sensor and three-axis magnetic sensors. A permanent magnet is installed as a magnetic source at the starting point of a continuous robot. Three posture sensors are installed on different connecting disk to detect its corresponding position and direction. Combining the position and direction of different connecting disk, the shape of continuum robot in 3D space can be reconstructed by piecewise curve-fitting method. The sensors are not distributed at equal intervals on continuum robot, so the shape sensing method is also applicable to continuum robot affected external load or other situations that do not satisfy constant curvature.

B. Shape Reconstruction Method

There is a preliminary study on this shape sensing method, o assuming that the position and direction $p= (x, y, z, m, n, p)$ of the specific connecting disk with posture have been acquired by the posture sensor, the shape sensing can be performed by the following shape reconstruction method.

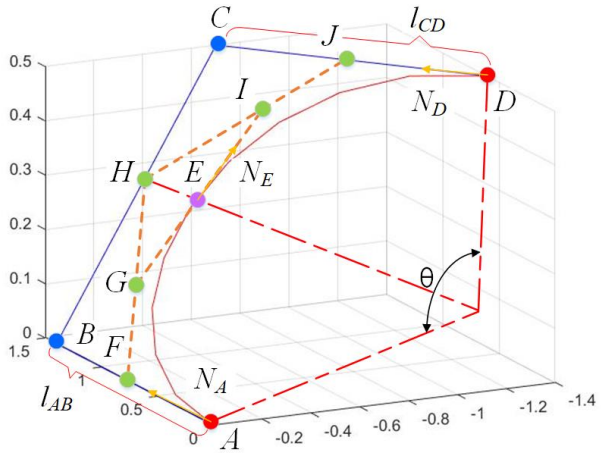

Figure 2. Cubic Bézier curve. *A* is the start point, and *D* is the end point, B and *C* is the control point. The curve starts at start point(*A*) going toward control point(*B* and *C*) and arrives at end point(*D*).

Cubic Bézier curve is shown in Figure 2, *A* is the start point, and D is the end point, B and C is the control point. The curve starts at start point(*A*) going toward control point(*B* and *C*) and arrives at end point(*D*). The explicit form of the curve is:

$$B_C(t)=(1-t)^3A+3t(1-t)^2B+3t^2(1-t)C+t^3D \quad (1)$$

The position and direction of point *A* are known. *D* is the position and direction of connecting disk with sensor, which is equal to $p= (x, y, z, m, n, p)$. So control points *B* and *C* can be expressed as:

$$\begin{cases} B = A + l_{AB} g T_A \\ D = C - l_{CD} g T_D \end{cases} \tag{2}$$

l_{AB} and l_{CD} represent the distance from point A to point B and from point C to point D respectively. T_A and T_D represent the direction vectors of point A and point D respectively. So this curve can be determined by solving two unknown parameters (l_{AB} and l_{CD}). In order to solve these two parameters, we need to establish an optimal objective function. Because the continuum robot does not move during bending process, its length will not change. Based on this characteristic, the optimal objective function can be established by using the length of the continuum robot. l_i is defined as the length of the spine in the i-th segment (the distance between the i-th connecting disk and the i-1-th connecting disk), and l_{si} is defined as the corresponding length of the curve. These two functions can be expressed as:

$$\begin{cases} l_i = L / n \\ l_{si} = \left\| B_i - B_{i-1} \right\| = \left\| B(\frac{i}{n}) - B(\frac{i-1}{n}) \right\| \end{cases} \tag{3}$$

where n represents the number of points used to estimate the length of a curve in Quadratic Bézier curve fitting, which is equal to half of the number of the connection disks, then the error estimation function f can be expressed as:

$$f = \sum_{i=1}^{n} (l_i - l_{si})^2 \tag{4}$$

Two unknown parameters (l_{AB} and l_{CD}) can be calculated by finding the optimal solution of the optimal objective function. The LM algorithm is used to optimize the two parameters. The shape of one segment of the continuum robot can be detected by the above method.

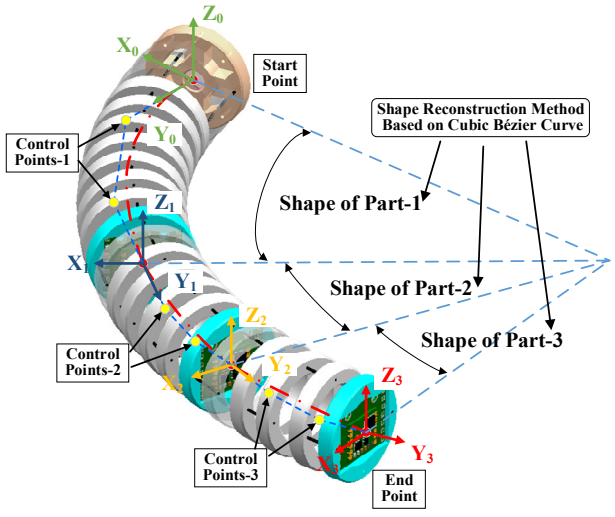

Figure 3. The shape of the continuum robot is divided into three parts by posture sensors. There are Shape of Part-1, Shape of Part-2 and Shape of Part-3, respectively. Each part will use shape reconstruction method based on cubic Bézier curve.

As shown in Figure 3, the shape of the continuum robot is divided into three parts by posture sensors. According to the method of piecewise fitting curves, the explicit form of the shape reconstruction is:

$$\begin{cases} B_{C1}(t) = (1-t)^3 A_1 + 3t(1-t)^2 B_1 + 3t^2(1-t) C_1 + t^3 D_1 \\ B_{C2}(t) = (1-t)^3 D_1 + 3t(1-t)^2 B_2 + 3t^2(1-t) C_2 + t^3 D_2 \\ B_{C3}(t) = (1-t)^3 D_2 + 3t(1-t)^2 B_3 + 3t^2(1-t) C_3 + t^3 D_3 \end{cases} \tag{5}$$

In this way, the shape of continuum robot can be reconstructed in 3D space even if the end of the robot is subjected to external load. In the next section, we will focus on the effect of external loading on bending curvature of the robot and how to arrange the sensors layout according to simulation analysis.

III. Effect of External Loading on Bending Curvature and Layout Scheme of Sensors

A. Effect of External Loading on Bending Curvature

Many researchers have found that the external load will change the shape of the continuum robot when they study its bending motion. In this chapter, the simulation analysis will be used to analyze how the curvature and radius of each section of the continuum robot will change, when the end of the bending continuum robot with constant curvature is subjected to external load, so as to determine the layout scheme of sensors.

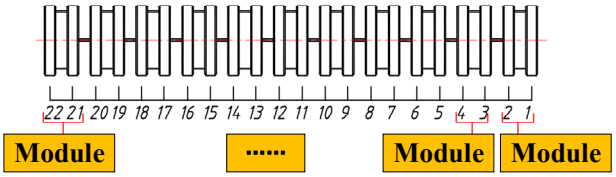

Figure 4. Marking the connecting disks of the continuum robot from 1 to 22. Starting with No.1 connection disk, each two adjacent connecting disks are defined as one set of module.

As shown in Figure 4, each connecting disk of the continuum robot is marked. Starting with No.1 connection disk, each two adjacent connecting disks are defined as one set of module according to the method shown in the Figure 4. There are 11 groups in total. The purpose of dividing modules is that the NiTi columns of each connecting disk are interlaced. If the continuum robot bends in a certain plane, only the columns between each module will bend. The concrete structure and bending motion mode are further elaborated in [21].

The 3D model of bending continuum robot with constant curvature is built as shown in Figure 5(a). The model is imported into the simulation software for force analysis. The starting point of the robot is fixed end, the end is subjected to external loads of 0.1N, 0.2N and 0.3N, respectively. The shape change of the continuous robot is shown in Figure 5(b)(c)(d). From the figure, we can draw a preliminary conclusion that the curvature from the end to the middle of the continuum robot has changed obviously.

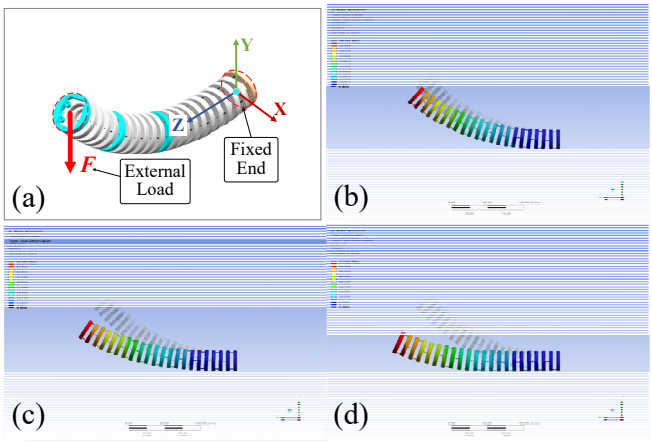

Figure 5. Simulation analysis of the continuum robot affected by external load. (a) The 3D model of bending continuum robot with constant curvature, The starting point of the robot is fixed end, the end is subjected to external loads (b) Deformation with 0.1N external load, (c) Deformation with 0.2N external load, (d) Deformation with 0.3N external load.

In order to get more detailed curvature change values, as shown in Figure 6, we use image recognition to analyze the curvature of the continuum robot under four different conditions(no external load, 0.1N, 0.2N and 0.3N external load), and mark the center of mass of each module with red dots .

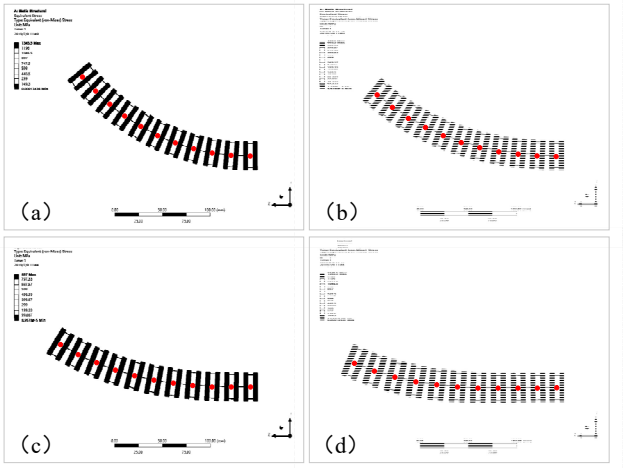

Figure 6. Centroids of the modules. (a) no external load, (b) 0.1N external load, (c) 0.2N external load, (d) 0.3N external load.

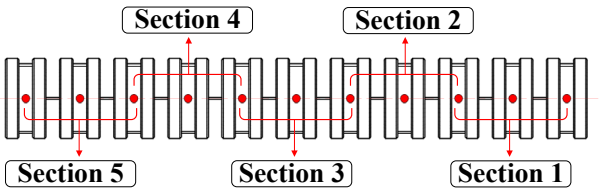

Figure 7. Section segmentation of the continuum robot. Each of three adjacent red dots is defined as one section, with a total of 5 sections.

In the way of [1], a concise method for image recognition to obtain the shape of the continuum robot is proposed, which is a shape reconstruction algorithm for a section of arc determined by three points. According to the methods mentioned in the above literature, the continuum robot is further divided into five sections by the marked red dots. The specific method is shown in Figure 7. The curvature and radius of each section can be obtained by the following methods

The expression of any circle in a plane can be defined as

$$(x-a_c)^2+(y-b_c)^2=r^2 \tag{6}$$

where (a_c, b_c) is the coordinate of the center of the circle and r is the radius of the circle, both of them are unknown. In order to solve unknown parameters, the following auxiliary parameters can be defined:

$$\alpha=a_c^2+b_c^2-r^2 \tag{7}$$

The formula (7) is substituted for the formula (6), and the result is obtained.

$$2xa_c+2yb_c-\alpha=x^2+y^2 \tag{8}$$

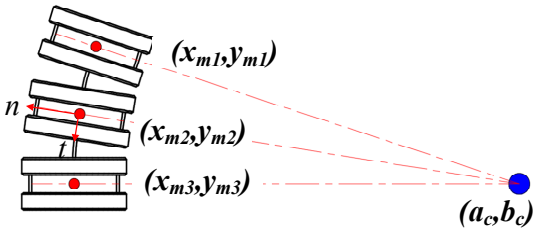

Figure 8. A shape reconstruction method for a section of arc determined by three points.

As can be seen from the Figure 8, there are three points in each section on this circle, so the following expressions can be obtained:

$$\begin{bmatrix} 2x_{m1} & 2y_{m1} & -1 \\ 2x_{m2} & 2y_{m2} & -1 \\ 2x_{m3} & 2y_{m3} & -1 \end{bmatrix}\begin{bmatrix} a_c \\ b_c \\ \alpha \end{bmatrix}=\begin{bmatrix} x_{m1}^2+y_{m1}^2 \\ x_{m2}^2+y_{m2}^2 \\ x_{m3}^2+y_{m3}^2 \end{bmatrix} \tag{9}$$

where (x_{mi},y_{mi}) is the centroid coordinate of the i-th module of each section. The radius and curvature of a circle can be obtained by transforming the formula (9). The expressions are as follows:

$$\begin{bmatrix} a_c \\ b_c \\ \alpha \end{bmatrix}=\begin{bmatrix} 2x_{m1} & 2y_{m1} & -1 \\ 2x_{m2} & 2y_{m2} & -1 \\ 2x_{m3} & 2y_{m3} & -1 \end{bmatrix}^{-1}\begin{bmatrix} x_{m1}^2+y_{m1}^2 \\ x_{m2}^2+y_{m2}^2 \\ x_{m3}^2+y_{m3}^2 \end{bmatrix} \tag{10}$$

$$K=\frac{1}{r} \tag{11}$$

According to the above method, the circles applicable to each region can be drawn. As shown in Figure 9, this figure shows the results of circle fitting routine in the case where the end of the continuum robot is subjected to an external load of 0.1N. In order to conveniently compare the circles applicable to each section after deformation, the coordinate system of the same scale is selected. It can be concluded that the change of

curvature and radius in Section 4 and Section 5 is more obvious than that in the previous three sections.

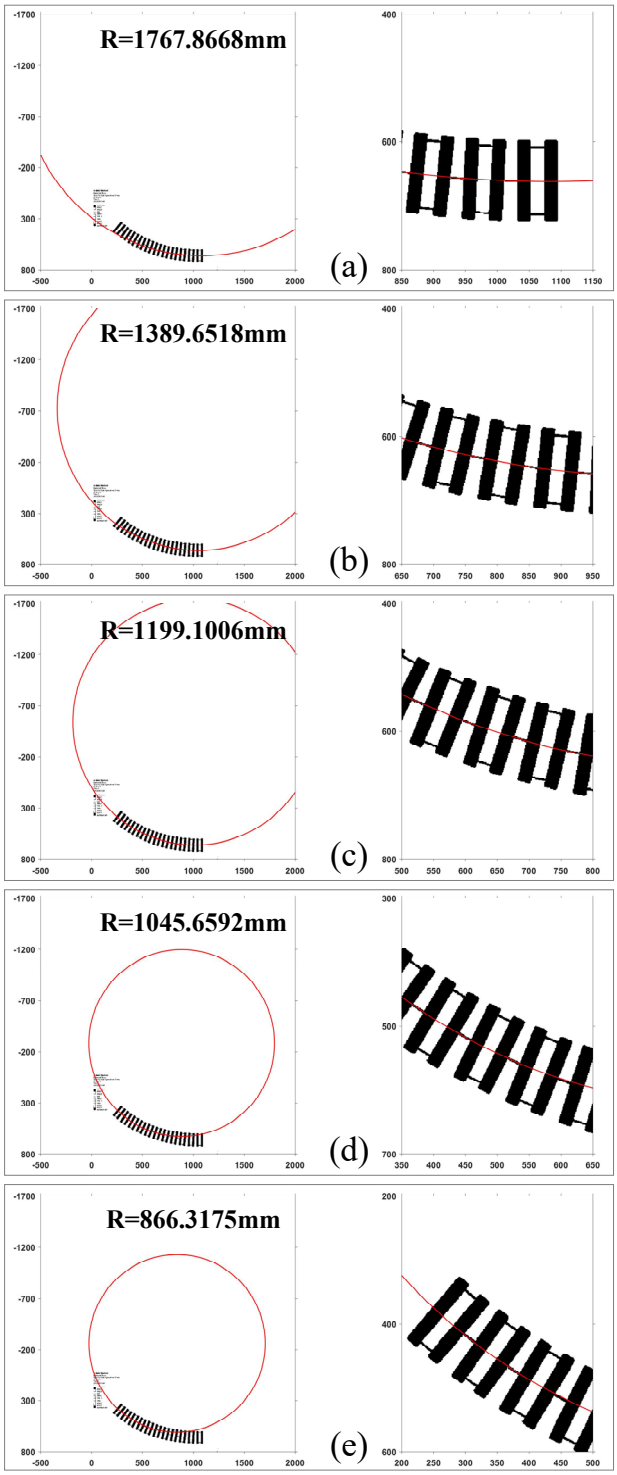

Figure 9. Results of circle fitting routine: (a) Circle fit to Section 1 and closeup of Section 1, (b) Circle fit to Section 2 and closeup of Section 2, (c) Circle fit to Section 3 and closeup of Section 3, (d) Circle fit to Section 4 and closeup of Section 4, (e) Circle fit to Section 5 and closeup of Section 5.

Table I, Table II and Table III show the radius and curvature of each section under three different external loads. We can draw the following conclusion: when the end of the continuum robot is subjected to external load, the shape and curve of each section will change. The larger the external load is, the more obvious the shape change is. The results show that the distance between sensors installed on continuum robot cannot be equal. Sensors should be installed according to the external loads applied on the robot.

TABLE I. THE RESULTING CURVATURES AND RADIUS (0.1N)

Section	K/10^{-4}	R/mm	ΔK
1	5.6565	1767.8668	0
2	7.1960	1389.6518	1.5395
3	8.3396	1199.1006	1.1436
4	9.5633	1045.6592	1.2237
5	11.5431	866.3175	1.9798

TABLE II. THE RESULTING CURVATURES AND RADIUS (0.2N)

Section	K/10^{-4}	R/mm	ΔK
1	3.4578	2891.9881	0
2	5.2381	1909.0778	1.7803
3	6.5022	1537.9510	1.2641
4	8.1056	1233.714	1.6034
5	11.1918	893.5139	3.0862

TABLE III. THE RESULTING CURVATURES AND RADIUS (0.3N)

Section	K/10^{-4}	R/mm	ΔK
1	0.9032	11071.5148	0
2	3.0681	3259.3470	2.1649
3	4.5869	2180.1119	1.5188
4	6.8370	1462.6240	1.7690
5	10.1815	982.1694	3.3445

B. Layout Scheme of Sensors

As shown in Figure 10, there is a line chart drawn from the data in the table. Section 3 is an inflection point of the curvature, which contains the middle position of the continuum robot. So the shape change of the continuum robot can be divided into two parts: the first part is the small deformation part from the starting point to the middle point of the continuum robot (including the Section 1, Section 2 and the first half of the Section 3). The second part is the large deformation part from the midpoint to the end point (including the second half of the Section 3, Section 4 and Section 5).

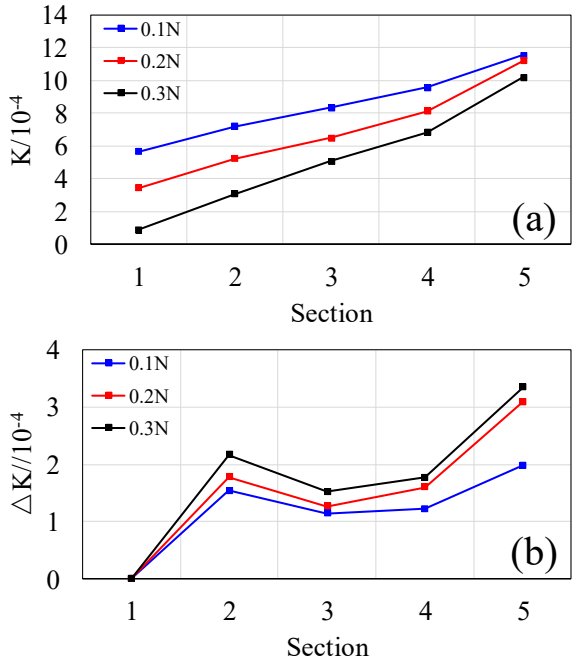

Figure 10. The line chart based on the resulting curvatures. (a) Curvature of each section in three cases (b) The deviation of curvature of each section in three cases.

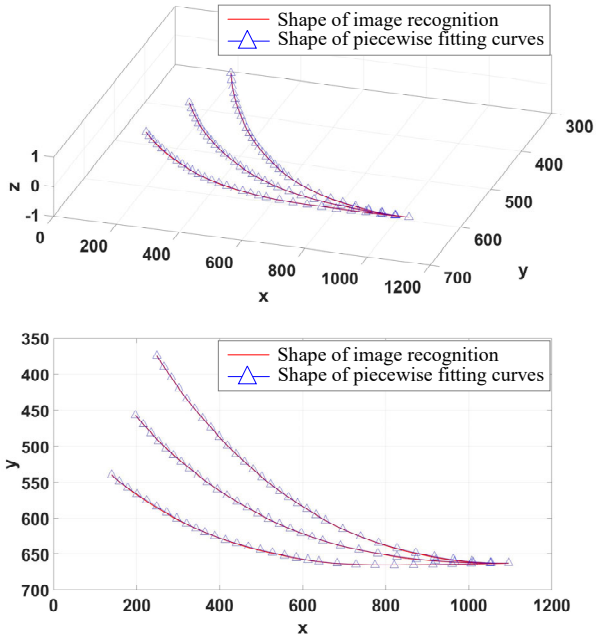

Figure 11. The shape of image recognition is compared with the shape of piecewise fitting cubic Bézier curves. Blue '—Δ—' represents the shape using the method of piecewise fitting curves. Red '—' represents the shape using the method of image recognition.

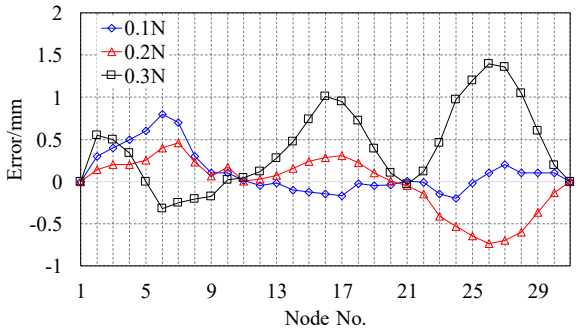

Figure 12. Shape sensing errors. For each part in Figure 11, distance error of each tracking node between the method of image recognition and the method of piecewise fitting curves has been shown

According to the above two parts of continuum robot, one sensor will be in-stalled in the first part, and two sensors will be installed in the second part. There are two main reasons for not using more sensors: one is to prevent data redundancy, the other is to prevent long processing time and affect real-time performance. The specific installation position of the sensor is as follows: the first sensor is mounted on the 11th connecting disk. The shape of the first part will be reconstructed through one fitting curve. The second sensor will be mounted on the 17th connecting disk. The third sensor will be mounted on the 22nd connecting disk. The shape of the second part will be reconstructed through two fitting curves.

The shape of image recognition is compared with the shape of piecewise fitting cubic Bézier curves after determining the layout scheme of sensors. The position and direction of the 11th, 17th and 22nd connecting disks under three kinds of external loads (0.1N, 0.2N and 0.3N) can be extracted from Fig.6. By substituting these data into the formula (5), we can get the shape of the continuum robot reconstructed by the method of piecewise fitting curves, which is the blue '— Δ —' shown in Figure 11. The shape of image recognition is the red '—' shown in Figure 11. ' Δ 'represents the tracing nodes on three fitting Bézier curves, and there are 11 tracing nodes on each Bézier curve. The corresponding tracing nodes are marked on the shape of image recognition, and then the tracing points under these two shape sensing methods are compared, which can be seen in Figure 12.The results show that the maximum distance error is 1.4 mm and the minimum distance error is 0.006 mm. The simulation results show that the layout scheme of sensors can achieve the piecewise curve fitting, and the shape of continuum robot affected by external load can be sensed accurately, even if the robot has large deflection.

IV. Conclusion

In this paper, a new method of shape sensing for continuum robot affected by external load is proposed. This scheme will integrate posture sensors into continuum robot, and then the shape of continuum robot affected by external load is reconstructed by fitting Bézier curve several times.

This paper focuses on how to arrange sensors according to the simulation analysis of continuum robot affected by external load to ensure the simplicity of configuration and the accuracy of shape sensing, so the Chapter-Ⅲ is an important chapter of this paper. In this chapter, firstly, the simulation analysis is used to analyze how the curvature and radius of each section of the continuum robot will change, when the end of the bending continuum robot with constant curvature is subjected to external load. Here we use shape sensing of image recognition to help us get the resulting curvatures and radius. Secondly, the layout scheme of sensors is determined according to the above

results of curvatures and radius, then the shape of image recognition is compared with the shape of piecewise fitting cubic Bézier curves. The results show that the maximum tracking error is 1.4 mm and the minimum tracking error is 0.006 mm. The simulation results verify the accuracy and feasibility of this method.

There are still some shortcomings in this paper. Firstly, this paper only makes a preliminary study on the method. The selection of sensors has not been implemented, and the accuracy of the method has not been verified by experiments. Secondly, only considering the single direction external load of the continuum robot, which results in the large deflection of the continuum robot only in a certain plane, we need to further study the influence of the external loads in different directions on the shape of the continuum robot in 3D space.

ACKNOWLEDGMENT

Research supported by National Natural Science Foundation of China (No. 51575256) and (No. 61973335), Natural Science Foundation of Jiangsu Province under Grant BK20191272, and "the Fundamental Research Funds for the Central Universities. NO. NS2018033".

REFERENCES

[1] M.W. Hannan, I. D. Walker, "Real-time shape estimation for continuum robots using vision," *Robotica*, 2005, 23(5): 645 – 651.

[2] C. L. Chen, C. L. Tai, Y.F. Lio, "Virtual binocular vision systems to solid model reconstruction," *International Journal of Advanced Manufacturing Technology*, 2007, 35(3-4):379-384.

[3] J. M. Croom, D. C. Rucker, J. M. Romano, et al., "Visual sensing of continuum robot shape using self-organizing maps," *Robotics and Automation (ICRA), 2010 IEEE International conference on. IEEE*, 2010, 4591-4596.

[4] C. V. Stewart, C. R. Dyer, "The Trinocular General Support Algorithm: A Three-camera Stereo Algorithm For Overcoming Binocular Matching Errors," *Computer Vision., Second International Conference on IEEE*, 1989:134-138.

[5] A. Vandini, C. Bergeles, F. Y. Lin, et al., "Vision-based intraoperative shape sensing of concentric tube robots," *IEEE/RSJ International Conference on Intelligent Robots and Systems. IEEE*, 2015:2603-2610.

[6] Y. L. Park, S. Elayaperumal, B. Daniel, S. C. Ryu, M. Shin, J. Savall, R. J. Black, B. Moslehi, M. R. Cutkosky, "Real-time estimation of 3-d needle shape and detection for mri-guided interventions," *IEEE/ASME Trans. Mechatronics.* 2010,15(6):906–915

[7] Y. Shapiro, G. Kosa, A. Wolf, "Shape tracking of planar hyper-flexible beams via embedded PVDF deflection sensors," *IEEE/ASME Trans. Mechatronics*. 2014, 19(4):1260-1267.

[8] M. Cianchetti, F. Renda, A. Licofonte, et al., "Sensorization of continuum soft robots for reconstructing their spatial configuration," *IEEE Ras & Embs International Conference on Biomedical Robotics and Biomechatronics. IEEE*, 2012:634-639.

[9] K. Suzumori, M. Mihara, S. Wakimoto, "Beautiful Flexible Microactuator changing its structural color with variable pitch grating," *IEEE International Conference on Robotics and Automation. IEEE*, 2011:2771-2776.

[10] Z. Chen, Y. Shen, N. Xi, X. Tan, "Integrated sensing for ionic polymer-metal composite actuators using PVDF thin films," *Smart Materials and Structures*, 2007 (16):262-271.

[11] Y. Bahramzadeh, M. Shahinpoor, "Dynamic curvature sensing employing ionic-polymer-metal composite sensors," S*mart Materials and Structures*, 2011 (20), 094011.

[12] S. Song, Z. Li, Q. H. Meng, et al., "Real-Time Shape Estimation for Wire-Driven Flexible Robots With Multiple Bending Sections Based on Quadratic Bézier Curves," *IEEE Sensors Journal*, 2015, 15(11):6326-6334.

[13] S. Song, C. Zhang, L. Liu, M. Meng, "Preliminary study on magnetic tracking-based planar shape sensing and navigation for flexible surgical robots in transoral surgery: methods and phantom experiments," *Int. J.Comput. Assist. Radiol. Surg*. 13 (2) (2018) 241–251.

[14] M.A. Davis, A. D. Kersey, J. Sirkis, et al., "Shape and vibration mode sensing using a fiber optic Bragg grating array," *Smart Materials and Structures*.1996 (6):759-765.

[15] R. J. Roesthuis, M. Kemp, J.J.V.D. Dobbelsteen, et al., "Three-Dimensional Needle Shape Reconstruction Using an Array of Fiber Bragg Grating Sensors," IEEE/ASME Trans. Mechatronics. 2014, 19(4):1115-1126.

[16] R. J. Roesthuis, S. Misra, "Steering of Multisegment Continuum Manipulators Using Rigid-Link Modeling and FBG-Based Shape Sensing," *IEEE Transactions on Robotics*, 2017, 32(2):372-382.

[17] H. Liu, A. Farvardin, R. Grupp, R. J. Murphy, R. H. Taylor, I. Iordachita, et al., "Shape Tracking of a Dexterous Continuum Manipulator Utilizing Two Large Deflection Shape Sensors," *IEEE Sensors Journal,* vol. 15, pp. 5494-5503, 2015

[18] R. Xu, A. Yurkewich, R. V. Patel, "Shape sensing for torsionally compliant concentric-tube robots," *International Society for Optics and Photonics*, 2016, pp. 97020V-97020V-8.

[19] D. C. Rucker, B.A. Jones and R.J. Webster III, "A Geometrically Exact Model for Externally Loaded Concentric-Tube Continuum Robots," *IEEE Transactions on Robotics*, 2010. 26(5): p. 769-780..

[20] X. Dong, M. Raffles, S. C. Guzman, et al., "A Novel Snake Arm Robot Using Twin-Pivot Compliant Joints: Design, Modeling and Validation," *Journal of Mechanisms & Robotics*, 2016, 8(2).

[21] X. Dong, D. Axinte, D. Palmer, et al., "Development of a slender continuum robotic system for on-wing inspection/repair of gas turbine engines," *Robotics & Computer Integrated Manufacturing*, 2017, 44(C):218-229.